Disdrometer measurements under Sense-City rainfall simulator

Auguste Gires[1], Philippe Bruley[2], Anne Ruas[2], Daniel Schertzer[1], and Ioulia Tchiguirinskaia[1]

[1]HM&Co, Ecole des Ponts, UPE, Champs-sur-Marne, France
[2]COSYS, IFSTTAR, Champs-sur-Marne, France

Correspondence: Auguste Gires (auguste.gires@enpc.fr)

Abstract.

The Hydrology, Meteorology and Complexity laboratory of Ecole des Ponts ParisTech (hmco.enpc.fr) and the Sense-City consortium (http://sense-city.ifsttar.fr/) make available a data set of optical disdrometers measurements coming from a campaign that took place in September 2017 under the rainfall simulator of the Sense-City climatic chamber which is located near
5 Paris. Two OTT Parsivel[2] were used. The size and velocity of drops falling through the sampling area of the devices of roughly few tens of cm^2 is computed by disdrometers. This enables to estimate the drop size distribution and further study rainfall micro-physics or kinetic energy for example. Raw data, i.e. basically a matrix containing a number of drops according to classes of size and velocity, along with more aggregated ones such rain rate or drop size distribution with filtering is available.

Link to the data set (Gires et al., 2019): http://doi.org/10.5281/zenodo.3347051

1 Introduction

Numerous rainfall simulators have been developed and used primarily to study soil erosion as well as tillage techniques. Indeed the natural extreme variability of rainfall features (occurrence, intensity, duration, drop size distribution...), makes more complicated such study under natural conditions. For a short historical review of rainfall simulators and their uses, the interested
15 reader is referred to Hall (1970). Rainfall simulators exhibit a wide range of complexity in terms of functioning enabling to reproduce more or less the properties of rainfall features depending on the aim of the study and the means available. Systems range from simple ones made of a network of few nozzles of various complexity (Olayemi and Yadav, 1983; Auerswald et al., 1992; Humphry et al., 2002; Paige et al., 2004; Parsons et al., 1998), to ones using disc-type water distributor hypodermic tube and needles in an attempt to reproduce not only a more or less uniform rainfall but also DSD and fall velocity of drops
20 (Abd Elbasit et al., 2010).

Some authors analysed the rain simulated with the help of disdrometers which are devices giving access to size and velocity of the falling drops. For example Meshesha et al. (2016) used such set up to investigate the relation between Kinetic Energy (KE) and rain rate (R), while Salles and Poesen (2000) showed that D^4V (where D is the diameter of drops and V their

velocity) was a better indicator for characterizing splash detachment than KE which is basically proportional to D^3V^2).
Iserloh et al. (2012) upgraded a portable rain simulator to investigate in details the processes of runoff generation and erosion.

In this paper we present disdrometer data collected during a measurement campaign aiming at testing a rainfall simulator installed in the climatic chamber of the Sense-City experiment. The campaign took place in September 2017. Before going,
5 it should mentioned that the two devices used here are already presented in Gires et al. (2018a) which deals with a previous campaign involving other instruments as well. Hence only the required basic elements on their functioning will be reminded here, while the reader is referred to the previous paper for more details as well as a longer discussion on the potential uses of such data. To the knowledge of the author such disdrometer data of rainfall simulators is not available to the community.

Data and methods are presented in section 2 with a brief reminder on the devices functioning and available data sets as well
10 a description of the rainfall simulator and the measurement campaign. Section 3 presents the data base and the available tools to use it. Outputs of the campaign are discussed in section 4 along with an illustrative comparison with some actual rainfall.

2 Data and methods

2.1 Brief reminder of the devices functioning and available datasets

As pointed out in the introduction, the measurement campaign uses devices whose functioning has already been described in
15 details in Gires et al. (2018a), hence only a short presentation is made in this paper. The two devices are part of the TARANIS observatory (exTreme and multi-scAle RAiNdrop parIS observatory (Gires et al., 2015, 2018a, b) of the Fresnel Platform of Ecole des Ponts ParisTech (https://hmco.enpc.fr/Page/Fresnel-Platform/en). The two optical disdrometers used here are OTT Parsivel[2] (see Battaglia et al., 2010 or the device documentation OTT, 2014), which are occlusion ones. It means that they are made of a transmitter, which generates a laser sheet and a receiver aligned with the transmitter with a sampling area of
20 roughly 50 cm^2 in between. When a drop falls through it, the beam is partially occluded which results in a decrease of the signal reaching the receiver. The amplitude and the duration of the decrease in the received signal is then analysed to estimate the equivolumic diameter and the velocity.

The output provided is actually not directly the features of each individual drop, but a matrix containing the number of drops recorded during the time step Δt (here $\Delta t = 30\ s$) according to classes of equivolumic diameter (index i and defined by a
25 centre D_i and a width ΔD_i expressed in mm) and fall velocity (index j and defined by a centre v_j and a width Δv_j expressed in $m.s^{-1}$). The classes are listed in Table 1.

The three quantities analysed in the paper and made available in the corresponding data base are the rain rate R in $mm.h^{-1}$, the drop size distribution $N(D)$ in $m^{-3}.mm^{-1}$ ($N(D)dD$ is the number of drops per unit volume in m^{-3} with an equivolimic diameter between D and $D+dD$ in mm), and the Kinetic Energy KE in $J.m^{-2}.h^{-1}$. Equivalently, we could have worked on a
30 kinetic energy expressed per mm of rain (i.e. in KE in $J.m^{-2}.mm^{-1}$) which is simply equal to KE/R (see Angulo-Martínez

Table 1. Definition of the classes of particle size and velocity for the Parsivel[2].

	Particle diameter classes			Particle velocity classes	
Class	Diameter (mm)	Width (mm)	Class	Velocity (m.s^{-1})	Width (m.s^{-1})
1	0.062	0.125	1	0.05	0.1
2	0.187	0.125	2	0.15	0.1
3	0.312	0.125	3	0.25	0.1
4	0.437	0.125	4	0.35	0.1
5	0.562	0.125	5	0.45	0.1
6	0.687	0.125	6	0.55	0.1
7	0.812	0.125	7	0.65	0.1
8	0.937	0.125	8	0.75	0.1
9	1.062	0.125	9	0.85	0.1
10	1.187	0.125	10	0.95	0.1
11	1.375	0.25	11	1.1	0.2
12	1.625	0.25	12	1.3	0.2
13	1.875	0.25	13	1.5	0.2
14	2.125	0.25	14	1.7	0.2
15	2.375	0.25	15	1.9	0.2
16	2.75	0.5	16	2.2	0.4
17	3.25	0.5	17	2.6	0.4
18	3.75	0.5	18	3.0	0.4
19	4.25	0.5	19	3.4	0.4
20	4.75	0.5	20	3.8	0.4
21	5.5	1.0	21	4.4	0.8
22	6.5	1.0	22	5.2	0.8
23	7.5	1.0	23	6.0	0.8
24	8.5	1.0	24	6.8	0.8
25	9.5	1.0	25	7.6	0.8
26	11.0	2.0	26	8.8	1.6
27	13.0	2.0	27	10.4	1.6
28	15.0	2.0	28	12.0	1.6
29	17.0	2.0	29	13.6	1.6
30	19.0	2.0	30	15.2	1.6
31	21.5	3.0	31	17.6	3.2
32	24.5	3.0	32	20.8	3.2

and Barros 2015 for a discussion on the use of both). The studied quantities are obtained for each time step from the raw matrix with the help of the following expressions:

$$R = \frac{\pi}{6\Delta t} \sum_{i,j} \frac{n_{i,j} D_i^3}{S_{eff}(D_i)} \tag{1}$$

$$N(D_i) = \frac{1}{S_{eff}(D_i)\Delta D_i \Delta t} \sum_j \frac{n_{i,j}}{v_j} \tag{2}$$

5 $$KE = \frac{\rho_{wat}\pi}{6\Delta t} \sum_{i,j} \frac{n_{i,j} D_i^3 v_j^2}{S_{eff}(D_i)} \tag{3}$$

where $S_{eff}(D_i)$ is the sampling area of the device. In the data presented in the paper for the Parsivel[2], we used $S_{eff}(D_i) = L(W - \frac{D_i}{2})$ where L = 180 mm and W = 30 mm are respectively the length and width of the sampling area (LW = 54 cm^2) (OTT, 2014). Since there is no modification on the raw data, the user can chose other approaches. It is a discrete DSD $N(D_i)$ that is computed, in which $N(D_i)\Delta D_i$ gives the number of drops with a diameter in the class i per unit volume (in m^{-3}).

10 $\rho_{wat} = 10^3 \ kg.m^{-3}$ is the volumic mass of water.

Finally it should be mentioned that no filter was implemented on the matrix for this specific implementation, i.e. the whole matrix is used. In some case authors introduced a filter to exclude drops whose measured fall velocity was too far from the theoretical expected terminal fall velocity and hence assumed to correspond to non meteorological hydrometeors (Gires et al., 2018a; Thurai and Bringi, 2005; Jaffrain and Berne, 2012). Again, since the raw matrices are made available, users can chose

15 to implement a filter if they want.

2.2 Description of the rainfall simulator

Sense-city is a 400 m^2 climate chamber funded by the French Research Agency. It allows the programmation of climate (temperature and humidity) as well as sun and rain. A tiny city is built inside the climate chamber to study different component of the city. The main research subjects are nano and micro sensors conception, air and water pollution, energy and the impact

20 of materials and vegetation on climate and pollution under different climate.

The rainfall simulator does not cover all the areas but only a 25 m^2 rectangular portion (3 m x 8.3 m, see figure 1). Two modes of rain are available : light and heavy rain. Each of them are produced by different injection nozzles. These nozzles are characterized through the angle of their internal cone. There are 12 nozzles with an angle of 90° for light rain and 12 nozzles with an angle of 120° for heavy rainfall. The nozzles are located at a 8 m height. The water flow can varie from 7 to 14 $l.min^{-1}$

25 for the light rain, and from 11 to 20 $l.min^{-1}$ for the heavy rain. The water flow is fixed for each simulation and is not supposed to varie more than 2 %. The water used is the drinking water.

2.3 Measurement campaign

The measurement campaign took place on 26-28 September 2017 in the Sense-City climatic chamber. Some pictures illustrating it can be found in Fig. 1. An overview of the set up is visible in Fig. 1.a where the area normally covered by the rainfall simulator was identified by the four metallic squares. The rainfall simulator, with its two separate networks for light and heavy rainfall was highlighted in yellow. A zoom on respectively the rainfall simulator and the two disdrometers used can be found in Fig. 1.b and .c.

Measurements were carried out for both light and heavy rainfall at five different locations within the area wet by the rainfall as shown in Fig. 2. The precise timing in local time of each test can be found in Tab. 2. Each test lasted at least 15 min. It takes few minutes at the beginning to reach a steady state.

In addition, a specific test keeping the disdrometers at location #1 while changing the input flow of water was carried out on 27-09-2017 between 09:45:00 and 11:20:00. Given that the rainfall simulator is not designed for such use, it resulted in a malfunctioning of the nozzles, notably with very large drops falling on the wet area. Hence measurement during this period are not discussed in this paper and should not be considered.
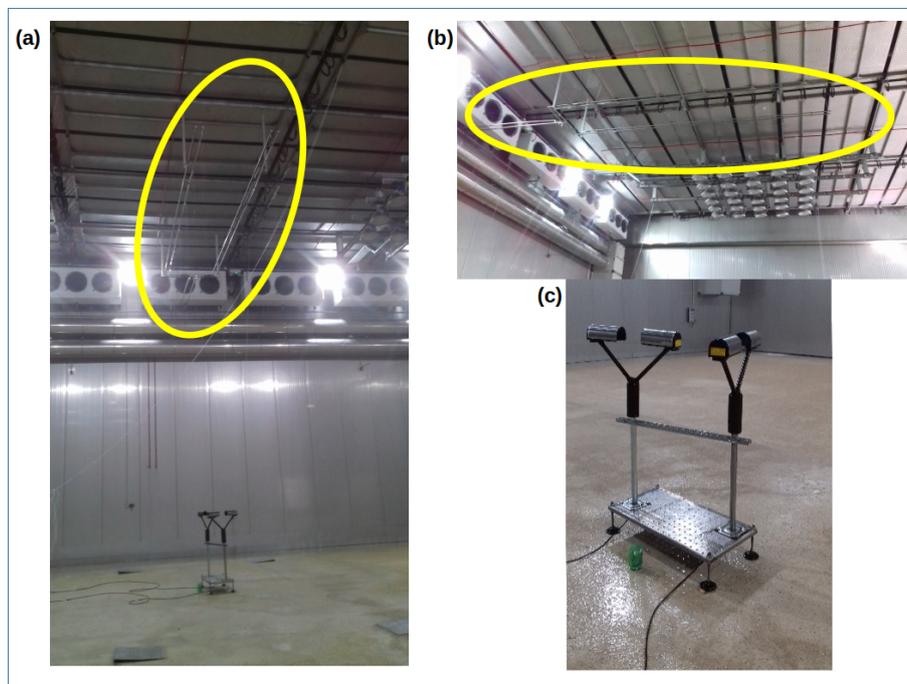
Figure 1. Pictures showing an overview of the measurement campaign (a), and a zoom on the rainfall simulator (b) and the disdrometers (c)
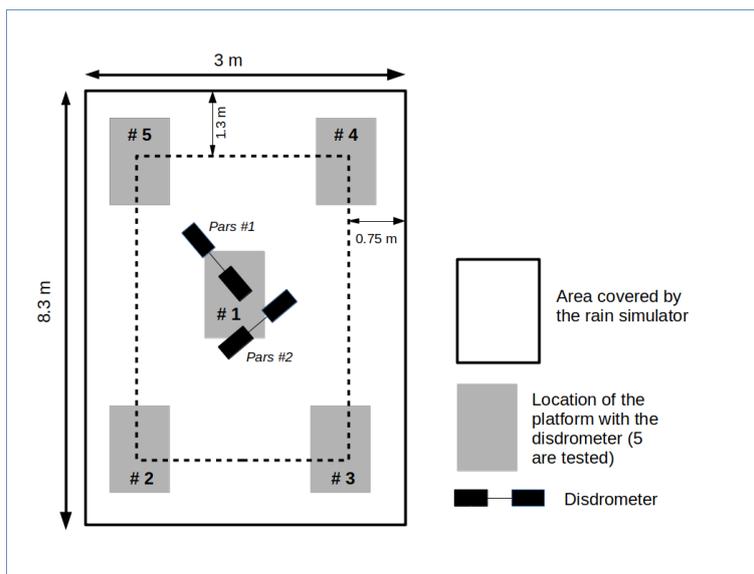
Figure 2. Scheme of the various locations tested over the area covered by the rainfall simulator

Table 2. Start and end time of tests for each location in both light and heavy rainfall configuration. Local time is used.

Light rainfall			Heavy rainfall		
Location	Start	End	Location	Start	End
1	2017-09-28 13:22:00	2017-09-28 14:07:00	1	2017-09-26 15:10:00	2017-09-26 15:43:00
2	2017-09-28 14:12:00	2017-09-28 14:33:00	2	2017-09-27 08:21:00	2017-09-27 09:05:00
3	2017-09-28 14:34:00	2017-09-28 14:54:00	3	2017-09-26 15:49:00	2017-09-26 16:26:00
4	2017-09-28 14:55:00	2017-09-28 15:15:00	4	2017-09-26 14:27:00	2017-09-26 15:05:00
5	2017-09-28 15:16:00	2017-09-28 15:34:00	5	2017-09-27 09:07:00	2017-09-27 09:40:00

3   Database

This section is actually quite similar to the corresponding one of Gires et al. (2018a). It contains a description of the data base content along with some available scripts. The data set for this campaign can be found at http://doi.org/10.5281/zenodo.3347051 (Gires et al., 2019). The main differences are the addition of the computation of KE and changes in the calendar which does not provides links to daily data but to individual tests. The data base is organized as follow:

    disdrometers_data_base/

        Raw_data_zip/

            Pars1/

            Pasr2/

            Each folder contains the files for its disdrometers.

            The name is Raw_DisdroName_YYYYMMDD.zip (ex : Raw_pars1_20170926.zip)

        Daily_data_python/

            Pars1/

            Pasr2/

            Each folder contains the files for its disdrometers.

            The name is DisdroName_raw_data_YYYYMMDD.csv (ex : Pars1_raw_data_20170926.npy)

        Exports/

            Full_matrix/

            KE/

            R/

            Each folder contains the files for all the disdrometers.

            The name is DisdroName_DataType_date.csv (ex : Pars1_KE_30_sec_2017_09_26_00_00_00__2017_09_26_23_59_30)

        Calendars/

            Data_5_min/ (one file per day, ex: R_5_min_Sense_City_2017_09_26_00_00_00__2017_09_26_23_59_30.csv)

            Data_30_sec/ (one file per day, ex: R_30_sec_Sense_City_2017_09_26_00_00_00__2017_09_26_23_59_30.csv)

            Quicklooks/ (one file per day and test, ex : Quicklook_Sense_City_2017_09_26_00_00_00__2017_09_26_23_59_30.png)

            Calendar_Sense_City.html

        Python_scripts/

            It contains the python scripts (and associated files) to generate and use this data base.

        Read_me.txt

            It contains a short description of the Taranis Sense-City data base.

3.1 "/Calendars"

Fig. 3 displays a snapshot of the page "Calendar_Sense_City.htlm" of the data base. It summarizes the campaign, and gives access to quicklooks of the measurements for each location and rainfall intensity. These quicklooks can also be directly accessed in the folder Quicklooks/. It also enables to access the daily quicklooks for each day (there are obviously numerous missing data, since disdrometers were only turned on during the actual tests), as well as of the corresponding rainfall times series with 30 second and 5 min time steps. These files can also directly be accessed in the folders Data_30_sec/ and Data_5_min/.

5   An example of quicklook can be found in Fig. 4 which is plotted for the test in location #1 with light rainfall. It aims at providing the user with an overview of the test. Quicklook's file name contain the name of the measurement campaign as well as the date and time of the start and end of the period it is covering. For example the file displayed in Fig. 4 is called "Quicklook_Sence_City_2017_09_28_13_22_00__2017_09_28_14_07_00.png", which means that it corresponds to the quicklook of "Sense-City" campaign between 2017-09-28 13:22:00 and 2017-09-28 14:07:00. A quicklook contains the

10   following graphs : (1) The rain rate R (in $mm.h^{-1}$) vs. time (in h) (upper left); (2) Cumulative rainfall depth C (in mm) vs. time (in h) (upper right); (3); The DSD $N(D)$ (in $m^{-3}.mm^{-1}$) vs. time (in h) (middle left); (4) Time series of missing time steps (a visible coloured bar for missing ones)(middle right); (5) A visual representation of the matrix containing the number of drops according the velocity and size classes, with the classes of velocity (resp. diameter) represented vertically (resp. horizontally); the solid black line is the curve corresponding to the relation between the terminal fall velocity of drops

15   as a function of their equivolumic diameter obtained by Lhermitte (1988) (middle right); (6) $N(D)D^3$ vs. D (lower left, $N(D)D^3$ and not simply $N(D)$ was plotted because it is proportional to the volume of rain obtained according to the drop diameter hence providing the reader a greater immediate insight of the contribution of each diameter class of drops to the observed rainfall amounts); (7) The temperature T (in ^oC) vs. time (in h). (8) The Kinetic Energy KE (in $J.m^2.h^{-1}$) vs. the rain rate R (in $mm.h^{-1}$). The solid line corresponds to a standard relation for rainfall $KE = 29R(1 - 0.72e^{-0.05R})$ found in

20   Angulo-Martínez and Barros (2015).

The files for daily rainfall rate are named in a similar way as the quicklooks except that "Quicklook" is replaced by "R_5_min" or "R_30_sec". They are in .csv files with the following format : (i) One line per time step (either 30 s or 5 min time step starting on YYYY-MM-DD 00:00:00 (local time). (ii) In each line, values of rain rate (in $mm.h^{-1}$) during this time step for the two disdrometers are separated with semi column and are preceded by a "nan;" (actually corresponding a

25   disdrometer not used in this campaign) and the order is nan;Pars#1;Pars#2; (iii) Missing data are noted as "nan".

3.2 "/Exports"

This folder contains exports in a simple .csv format of the main outputs of the disdrometer that could be relevant for potential users of this data, i.e. the full matrix of drops according to size and velocity classes (sub-folder "/Full_matrix"), kinetic energy (sub-folder "/KE") and rain rate (sub-folder "/R").

30   In a given folder, a file is typically called 'Pars1_KE_30_sec_2017_09_26_00_00_00__2017_09_26_23_59_30.csv' meaning the disdrometer name, the data type and start and end of the period corresponding to the data is easily visible for the user.

HM&Co disdrometers @ Sense-City

Here is a figure describing the configuration of the tests
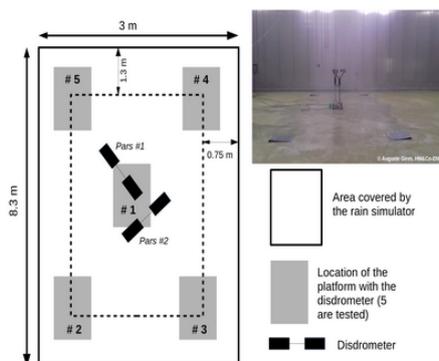
Quicklooks for each location and rainfall intensity

Light rainfall			Heavy rainfall		
Location	Start	End	Location	Start	End
1	2017-09-28 13:22:00	2017-09-28 14:07:00	1	2017-09-26 15:10:00	2017-09-26 15:43:00
2	2017-09-28 14:12:00	2017-09-28 14:33:00	2	2017-09-27 08:21:00	2017-09-27 09:05:00
3	2017-09-28 14:34:00	2017-09-28 14:54:00	3	2017-09-26 15:49:00	2017-09-26 16:26:00
4	2017-09-28 14:55:00	2017-09-28 15:15:00	4	2017-09-26 14:27:00	2017-09-26 15:05:00
5	2017-09-28 15:16:00	2017-09-28 15:34:00	5	2017-09-27 09:07:00	2017-09-27 09:40:00

Daily quicklooks and rainfall time series

Click on the link to download the data for the corresponding day. For the time series, it is a column sarting on YYYY-MM-DD 00:00:00 UTC and containing the successive 30 s (or 5 min) time steps. Missing data are noted as "nan". Column order is nan;Pars#1;Pars#2 (the first column contains only nan because it corresponds to a device that was not used during this measurement campaign).

2017-09-26	2017-09-27	2017-09-28
Quicklook	Quicklook	Quicklook
5 min series	5 min series	5 min series
30 sec series	30 sec series	30 sec series

Figure 3. Snapshot of the page "Calendar_Sense_City.htlm" of the data base.
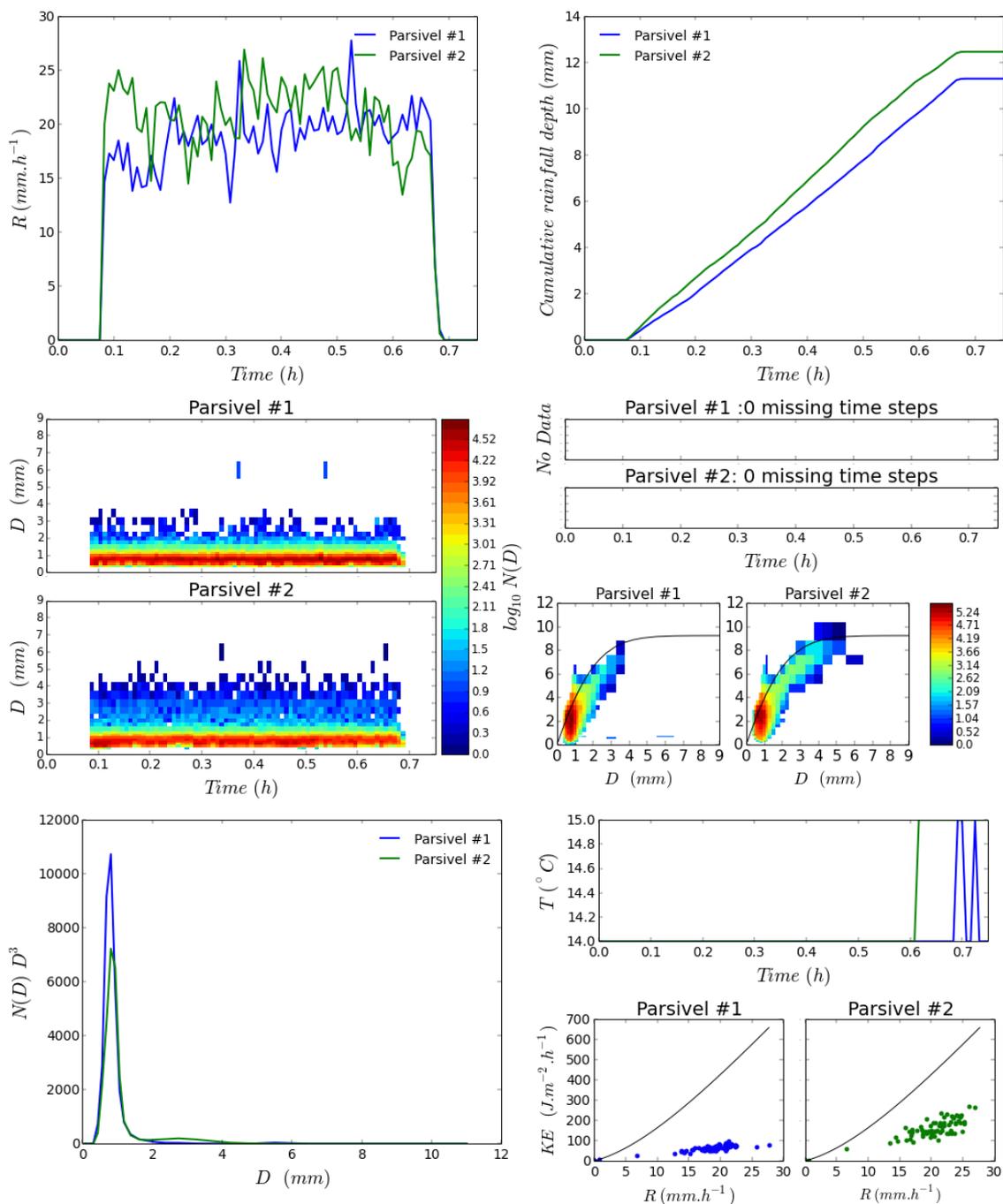
Figure 4. Quicklook of the measurements at the location #1 with light rainfall

In the file, the format is the following : (i) One line per time step; (ii) For each line : Date (YYYY-MM-DD HH:MM:SS); data. For R and KE data is simply the value for the corresponding time step. For the 'full matrix' it is : number of drops per class of velocity and size (1st size class - 1st velocity class,1st size class - 2nd velocity class, 1st size class - 2nd velocity class, ... , 2nd size class - 1st velocity class...) separated by comas (32 * 32 classes for Parsivel data). ex : 2017-09-26 17:27:00;0.0,0.0,0.0......,0.0 (iii) missing data are indicated as nan. These files are text files that can be read by any software.

3.3 "/Daily_data_python"

5   This folder contains the daily file for both disdrometers in there own sub-folder. Each file is stored in .npy format and requires Python 3 to be read. They contain the all the data collected stored as a list. It is these files that are read by the Python scripts described in the corresponding sub-section

3.4 "/Raw_data_zip"

This folder is actually very similar to the corresponding one of Gires et al. (2018a), so the description will simply be repeated.
10   "It contains a folder for each of the three disdrometers. Each of these folders contains a zip file for each day. This .zip file contains the data directly collected from the disdrometer. There is one text file for each 30 s time step. The precise format of these fields can be found in the Python scripts in the heading of the corresponding functions. This corresponds to the raw data. These data have been made available for expert users, but in practice it is believed that the .csv file or the Python scripts should be sufficient for most users."

15 3.5 Python scripts/

Again this section is very similar to the corresponding one of Gires et al. (2018a), with the addition of the function to export KE. This folder contains some Python scripts that can be used to carry out some initial analysis and data treatment with the data base. The tools are located in the script 'Tools_data_base_use_Sense_City_v4.py'. The main functions are (only a short description is given here - more details, including precise description of the inputs and outputs of the functions, are provided
20   as comments in each script) :

- Quicklook_and_R_series_generation_Sense_City_without_PWS : generating a quicklook image and the corresponding 30 s and 5 min rain rate time series for a given rainfall event for the Sense_City campaign.

- extracting_one_event_Sense_City : reading daily.npy files and generating three lists (one for each disdrometer) containing all the data that can be analysed for the Sense_City campaign.

25 - exporting_full_matrix : reading daily.npy files and exporting full matrix in .csv files for a given disdrometer and event

- exporting_R : reading daily.npy files and exporting R in .csv files for a given disdrometer and event

- exporting_T : reading daily.npy files and exporting T in .csv files for a given disdrometer and event

– exporting_KE : reading daily.npy files and exporting KE in .csv files for a given disdrometer and event

Commented examples of use of the functions can be found in the scripts : 'Example_of_use_data_base_sense_city.py'. Note that Python 3 (www.python.org) is required because the .npy files containing the data were saved using Python 3.

4   Discussion

4.1   Not homogeneous over the surface

Fig. 5 displays the average rain rate expressed in $mm.h^{-1}$ measured at each location (#) and disdrometer for both light and
5   heavy rainfall simulations. The first and last 5 min were not considered in the computation of the average. It appears that for both rainfall configurations, the rain rate is not uniform over the wet surface. This phenomenon is more pronounced for heavy rainfall, with even a strong disparity between the two disdrometers at location #1. In general and not surprisingly, there is a tendency for the average rain rate to decrease when disdrometers are located further from the centre.
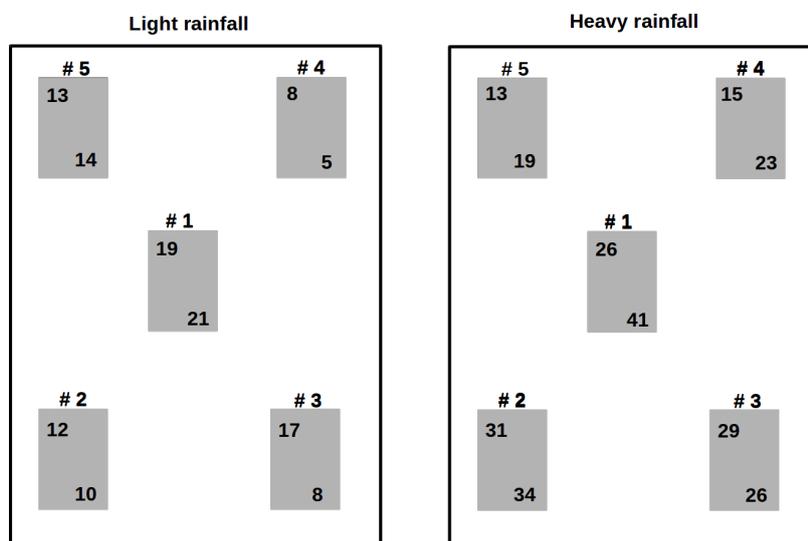
Figure 5. Average rain rate expressed in $mm.h^{-1}$ during for each location (#) for both light and heavy rainfall simulations

4.2   Some differences with regards to standard rainfall.

10   Fig. 4 and 6 display quicklooks of the measurements carried out at the location #1 with respectively light and heavy rainfall. As an illustration, Fig. 7 displays a similar quicklook for an actual rainfall event that occurred on 10 February 2019 between 07:00:00 and 10:00:00 (UTC time for this event). The disdrometers and configuration are the same as in Gires et al. (2018a). This event lasted 3 h and resulted in a total rainfall depth of roughly 6 mm. Limited rain rates lower than 10 $mm.h^{-1}$ were recorded during the whole event, except during roughly 10 min approximately 1 h after the beginning of the event.

15   The first point is the steadiness of the features of the simulated features both in terms of rain rate (upper left) or DSD (middle left), which is radically opposed to what is found in natural rainfall. It is actually a property that is wanted for a rainfall simulator. Let us simply mention that it takes few minutes to reach a "permanent" regime in the functioning of the nozzles.

A closer look at the DSD (middle left and lower left on the quicklooks) reveals that the drops generated by the rainfall simulators are smaller than actuals ones. More precisely the DSD is much thicker and centred on smaller drops. A common indicator is the mass-weighted diameter D_m expressed in mm which is equal to the ratio between the moment of order 4 and
5   3 of the DSD :

$$D_m = \frac{\int_0^{D_{max}} D^4 N(D) dD}{\int_0^{D_{max}} D^3 N(D) dD} \tag{4}$$

D_m was computed on average for the whole test in location #1 for both rainfall intensity. For light intensity it is equal to 0.99 and 0.88 mm for respectively Pars#1 and Pars#2. Considering each time step independently it varies within the range 0.95-1.05 mm for Pars#1 and within the range 0.85-0.90 for Pars#2. With regards to the tests for heavy rainfall, on average at
10   location #1 it is equal to 0.88 and 1.07 mm for respectively Pars#1 and Pars#2. Considering each time step independently it varies within the range 0.8-0.9 mm for Pars#1 and within the range 1.0-1.2 for Pars#2. These values are significantly smaller than typical ones for actual rainfall. For instance for the event displayed in Fig. 7, we find D_m equal to 1.51 and 1.41 for respectively Pars#1 and Pars#2 with variations between 0.8 and 3 mm during the event. Furthermore, D_m tends to increase with increasing rainfall intensities, so much greater values would be expected for rain rate generated with the simulator. It
15   should be noted that with the simulator very little differences are found for the shape of the DSD between simulations with either light or heavy intensities.

In addition, the maps basically displaying the number of drops according to the classes of velocities and sizes (middle right in the quicklooks) shows that drops tend to reach the disdrometers with lower velocities than expected. Indeed for actual rainfall, measured distribution is roughly scattered around the expected theoretical relation between the terminal fall velocity and the
20   equivolimic diameter (solid black line). Such measured distribution is shifted toward smaller velocities. It can be noticed that this issue is more pronounced for larger drops than small ones, which is expected. This is due to the fact the height of the rainfall simulator of 8 m is not sufficient to enable the drops to reach their terminal fall velocities. For instance Abd Elbasit et al. (2010) used a 12 m tower to ensure proper velocities for all sizes of drops.

As a result of both the absence of large drops and lower fall velocity, the kinetic energy of the simulated rainfall is strongly
25   underestimated with the regards to the expected values for such rain rates. This feature is visible on the lower right panel of the quicklooks of Fig. 4 and 6. The commonly found relationship is properly retrieved for the actual rainfall (Fig. 7).
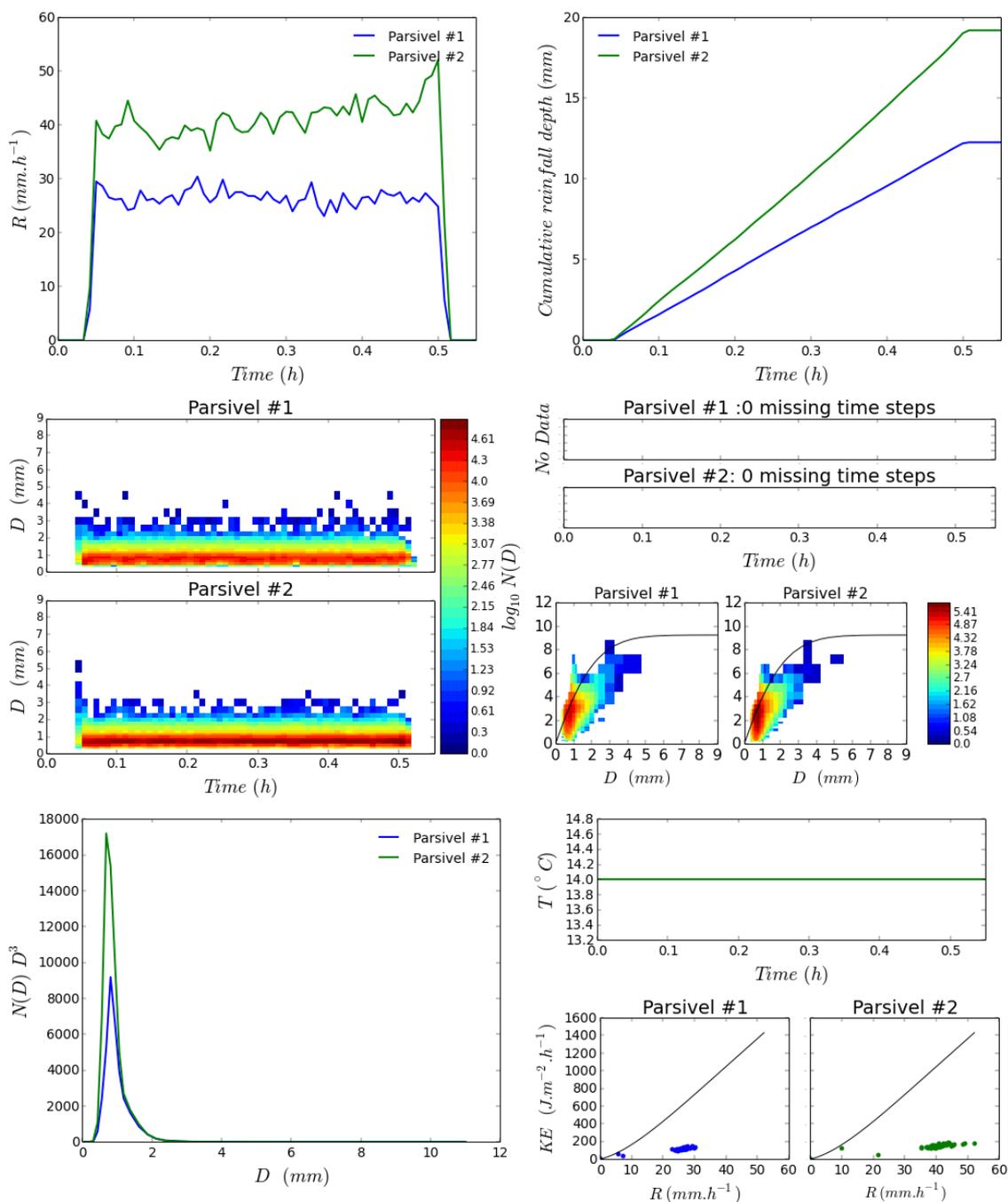
Figure 6. Quicklook of the measurements at the location #1 with heavy rainfall
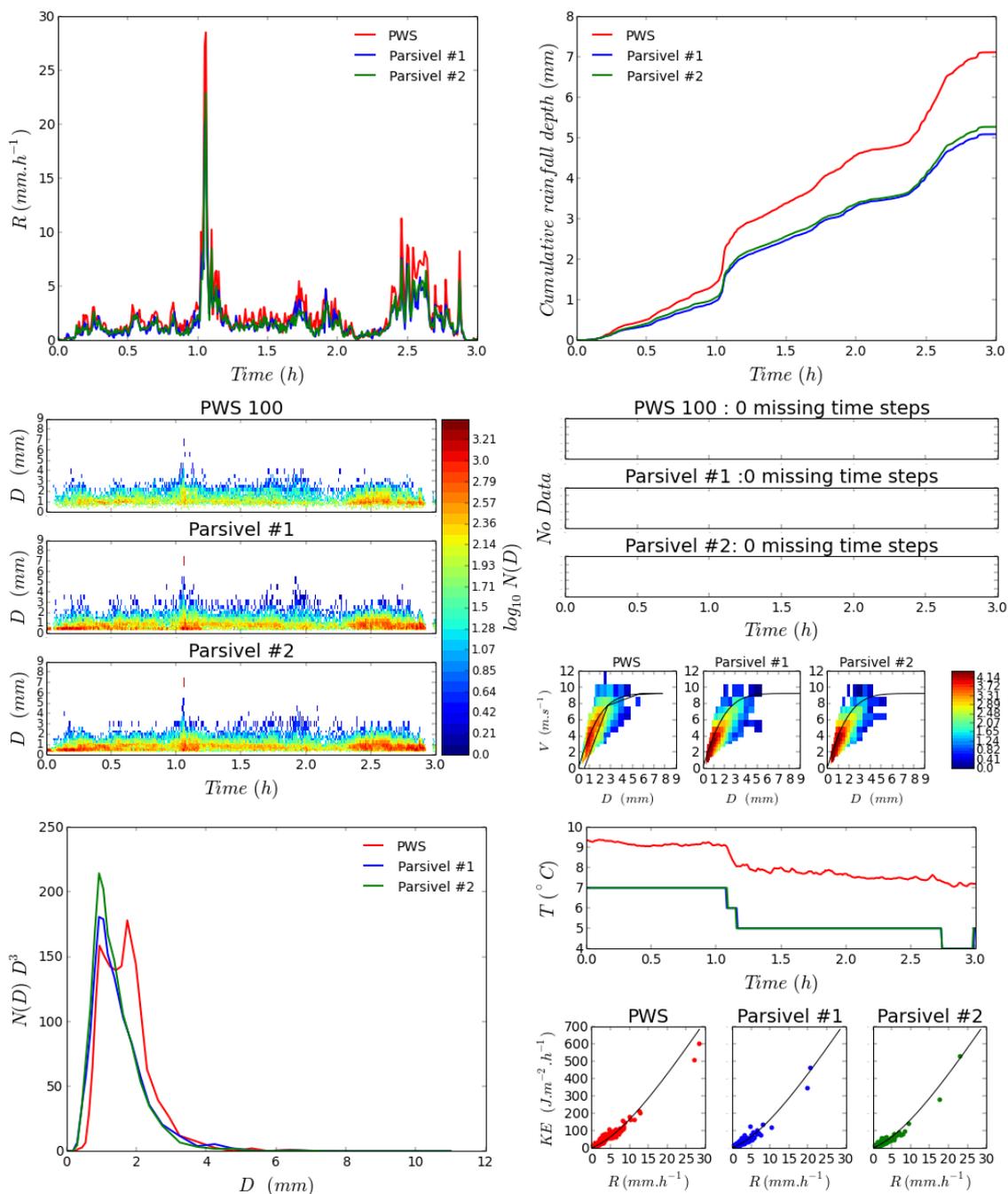
Figure 7. Quicklook of the measurements carried out on the roof of the Carnot building of ENPC campus on 10 February 2019 between 07:00:00 and 10:00:00 (UTC time)

5 Data availability

The data base presented in this paper has been made available by the Hydrology, Meteorology and Complexity laboratory of Ecole des Ponts ParisTech (HM&Co-ENPC) and the Sense-City consortium at https://doi.org/10.5281/zenodo.3347051. The
30 following citation should be used for every use of the data :

– For this paper : TO BE COMPLETED ONCE AVAILABLE

– For the data base : Gires et al. (2019), http://doi.org/10.5281/zenodo.3347051

This data set is available for download free of charge. License terms apply. Finally it should mentioned that these disdrometers and others have been and are used in other measurement campaign by HM&Co. Regular updates of their status along with
5 updates of the database are to be provided through the lab's website (hmco.enpc.fr). The web page https://hmco.enpc.fr/portfolio-archive/taranis-observatory/ contains links to summary calendars with access to quicklooks past and ongoing measurement campaigns (daily updates).

6 Conclusions

The 30 s disdrometer data from a measurement campaign beneath a rainfall simulator are presented in this paper. Raw data
10 as well as Python-formatted data with the associated scripts for basic manipulation are described and made available to the community for further use.

In order to discuss the features the rainfall generated by the simulator, an illustrative comparison is made with actual rainfall. It appears the properties of the rainfall generator remain steady over time which a wanted quality. In terms of more refined properties, the drop size distribution generated is thinner that actual rainfall and centred on smaller drops. In addition the height
15 of the simulator is not sufficient for larger drops (> 1 mm) to reach their terminal fall velocity. As a consequence the kinetic energy of the simulated rainfall is smaller that in actual rainfall for a similar rain rate. Depending on the applications, these observed features should be taken into account.

Competing interests. The authors declare that they have no conflict of interest.

Acknowledgements. The authors greatly acknowledge partial financial support from the Chair of Hydrology for Resilient Cities (endowed
20 by Veolia) of the Ecole des Ponts ParisTech, and the Ile-de-France region RadX@IdF Project. We also want to thank the ANR, the French Funding Agency, for supporting Sense City Equipe

References

Abd Elbasit, M. A. M., Yasuda, H., Salmi, A., and Anyoji, H.: Characterization of rainfall generated by dripper-type rainfall simulator using piezoelectric transducers and its impact on splash soil erosion, Earth Surface Processes and Landforms, 35, 466–475, https://doi.org/10.1002/esp.1935, https://onlinelibrary.wiley.com/doi/abs/10.1002/esp.1935, 2010.

Angulo-Martínez, M. and Barros, A.: Measurement uncertainty in rainfall kinetic energy and intensity relationships for soil erosion studies: An evaluation using PARSIVEL disdrometers in the Southern Appalachian Mountains, Geomorphology, 228, 28–40, https://doi.org/10.1016/j.geomorph.2014.07.036, http://www.sciencedirect.com/science/article/pii/S0169555X14004140, 2015.

Auerswald, K., Kainz, M., Schröder, D., and Martin, W.: Comparison of German and Swiss Rainfall Simulators - Experimental Setup, Zeitschrift für Pflanzenernährung und Bodenkunde, 155, 1–5, https://doi.org/10.1002/jpln.19921550102, https://onlinelibrary.wiley.com/doi/abs/10.1002/jpln.19921550102, 1992.

Battaglia, A., Rustemeier, E., Tokay, A., Blahak, U., and Simmer, C.: PARSIVEL Snow Observations: A Critical Assessment, Journal of Atmospheric and Oceanic Technology, 27, 333–344, http://dx.doi.org/10.1175/2009JTECHA1332.1, 2010.

Gires, A., Tchiguirinskaia, I., and Schertzer, D.: Multifractal comparison of the outputs of two optical disdrometers, Hydrological Sciences Journal, pp. null–null, https://doi.org/10.1080/02626667.2015.1055270, http://dx.doi.org/10.1080/02626667.2015.1055270, 2015.

Gires, A., Tchiguirinskaia, I., and Schertzer, D.: Two months of disdrometer data in the Paris area, Earth System Science Data, 10, 941–950, https://doi.org/10.5194/essd-10-941-2018, https://www.earth-syst-sci-data.net/10/941/2018/, 2018a.

Gires, A., Tchiguirinskaia, I., and Schertzer, D.: Pseudo-radar algorithms with two extremely wet months of disdrometer data in the Paris area, Atmospheric Research, 203, 216 – 230, https://doi.org/https://doi.org/10.1016/j.atmosres.2017.12.011, http://www.sciencedirect.com/science/article/pii/S0169809517307111, 2018b.

Gires, A., Bruley, P., Ruas, A., Schertzer, D., and Tchiguirinskaia, I.: Data for "Disdrometer measurements under Sense-City rainfall simulator", https://doi.org/10.5281/zenodo.3347051, 2019.

Hall, M. J.: A Critique of Methods of Simulating Rainfall, Water Resources Research, 6, 1104–1114, https://doi.org/10.1029/WR006i004p01104, https://agupubs.onlinelibrary.wiley.com/doi/abs/10.1029/WR006i004p01104, 1970.

Humphry, J. B., Daniel, T. C., Edwards, D. R., and N., S. A.: A Portable Rainfall Simulator for Plot–Scale Runoff Studies, Applied Engineering in Agriculture, 18, 199–204, https://doi.org/10.13031/2013.7789, 2002.

Iserloh, T., Fister, W., Seeger, M., Willger, H., and Ries, J.: A small portable rainfall simulator for reproducible experiments on soil erosion, Soil and Tillage Research, 124, 131 – 137, https://doi.org/https://doi.org/10.1016/j.still.2012.05.016, http://www.sciencedirect.com/science/article/pii/S0167198712001201, 2012.

Jaffrain, J. and Berne, A.: Quantification of the Small-Scale Spatial Structure of the Raindrop Size Distribution from a Network of Disdrometers, Journal of Applied Meteorology and Climatology, 51, 941–953, http://dx.doi.org/10.1175/JAMC-D-11-0136.1, 2012.

Lhermitte, R. M.: Cloud and precipitation remote sensing at 94 GHz, Geoscience and Remote Sensing, IEEE Transactions on, 26, 207–216, 1988.

Meshesha, D. T., Tsunekawa, A., Tsubo, M., Haregeweyn, N., and Tegegne, F.: Evaluation of kinetic energy and erosivity potential of simulated rainfall using Laser Precipitation Monitor, CATENA, 137, 237–243, https://doi.org/10.1016/j.catena.2015.09.017, http://www.sciencedirect.com/science/article/pii/S034181621530117X, 2016.

Olayemi, F. and Yadav, R.: Rainfall simulator for tillage research in the tropics, Soil and Tillage Research, 3, 397 – 405, https://doi.org/https://doi.org/10.1016/0167-1987(83)90041-7, http://www.sciencedirect.com/science/article/pii/0167198783900417, 1983.

5   OTT: Operating instructions, Present Weather Sensor OTT Parsivel2, 2014.

Paige, G., Stone, J., Smith, J., and Kennedy, J.: The Walnut Gulch Rainfall Simulator: A computer-controlled variable intensity rainfall simulator, ASAE Appl. Eng. Agric., 20, https://doi.org/10.13031/2013.15691, 2004.

Parsons, A. J., Stromberg, S. G. L., and Greener, M.: Sediment-transport competence of rain-impacted interrill overland flow, Earth Surface Processes and Landforms, 23, 365–375, https://doi.org/10.1002/(SICI)1096-9837(199804)23:4<365::AID-

10   ESP851>3.0.CO;2-6, https://onlinelibrary.wiley.com/doi/abs/10.1002/%28SICI%291096-9837%28199804%2923%3A4%3C365%3A% 3AAID-ESP851%3E3.0.CO%3B2-6, 1998.

Salles, C. and Poesen, J.: Rain properties controlling soil splash detachment, Hydrological Processes, 14, 271–282, https://doi.org/10.1002/(SICI)1099-1085(20000215)14:2<271::AID-HYP925>3.0.CO;2-J,   https://onlinelibrary.wiley.com/doi/abs/ 10.1002/%28SICI%291099-1085%2820000215%2914%3A2%3C271%3A%3AAID-HYP925%3E3.0.CO%3B2-J, 2000.

15   Thurai, M. and Bringi, V. N.: Drop Axis Ratios from a 2D Video Disdrometer, Journal of Atmospheric and Oceanic Technology, 22, 966–978, http://dx.doi.org/10.1175/JTECH1767.1, 2005.